

ANC-ERA: Random Access for Analog Network Coding in Wireless Networks

Wenguang Mao, Xudong Wang, *Senior Member, IEEE*, Aimin Tang, and Hua Qian

Abstract—Analog network coding (ANC) is effective in improving spectrum efficiency. To coordinate ANC among multiple nodes without relying on complicated scheduling algorithm and network optimization, a new random access MAC protocol, called ANC-ERA, is developed to dynamically form ANC-cooperation groups in an ad hoc network. ANC-ERA includes several key mechanisms to maintain high performance in medium access. First, network allocation vectors (NAV) of control frames are properly set to avoid over-blocking of channel access. Second, a channel occupation frame (COF) is added to protect vulnerable periods during the formation of ANC cooperation. Third, an ACK diversity mechanism is designed to reduce potentially high ACK loss probability in ANC-based wireless networks. Since forming an ANC cooperation relies on bi-directional traffic between the initiator and the cooperator, the throughput gain from ANC drops dramatically if bi-directional traffic is not available. To avoid this issue, the fourth key mechanism, called flow compensation, is designed to form different types of ANC cooperation among neighboring nodes of the initiator and the cooperator. Both theoretical analysis and simulations are conducted to evaluate ANC-ERA. Performance results show that ANC-ERA works effectively in ad hoc networks and significantly outperforms existing random access MAC protocols.

1 INTRODUCTION

ANALOG network coding (ANC) [1] or physical-layer network coding (PLNC) [2] was first proposed for a two-way relay channel to improve communication efficiency. With this technique, two end users concurrently transmit their data frames to the relay node, and then the superimposed signals are forwarded to end users. Since one of frames in the superimposed signals is known, the other frame can be extracted by either end user. Compared to one-way relaying and traditional network coding, ANC achieves better spectrum utilization and significantly enhances the network throughput performance [1], [3]. Thus, it is beneficial to apply ANC to wireless networks. Moreover, the recent progress in ANC research [4], [5], [6], [7] gradually leads to more practical ANC schemes that are not constrained by the synchronization, the modulation scheme, the frequency offset, or the frame size.

So far, a number of schemes have been developed to apply ANC to wireless networks with simple topologies such as line [8], star [9], layered topology [10], hierarchical topology [11], and other special relay structures [12]. However, for wireless networks with a general topology such as mesh networks and ad hoc networks, many problems still remain to be solved. Particularly, how to effectively form ANC cooperation among network nodes poses the most challenging problem. In [13], channel assignment and link scheduling for forming ANC cooperation groups in an ad

hoc network are formulated as an optimization problem, which is proved to be NP-hard. In general, the complexity of scheduling ANC cooperation groups in a wireless network is proved to be NP-complete in [14]. Therefore, for practical application of ANC in a general wireless network, random access becomes a preferred approach.

To the best of our knowledge, only a limited number of papers [15], [16], [17] have studied random access MAC protocols for ANC (or PLNC). In [15], an algebraic model is derived for the MAC layer and a random access algorithm is designed for ANC at a theoretical level; No practical MAC protocol is actually developed. In [16], a PLNC-based random access MAC protocol is developed to support concurrent transmissions of different communication pairs in a single-hop ad hoc network. In [17], a distributed MAC protocol is proposed to support ANC cooperation in general wireless mesh/ad hoc networks. This protocol enhances the network throughput performance in the scenarios where symmetrical bi-directional traffic flows are available, but loses its gain if such traffic pattern is absent. Actually, in many scenarios, e.g., wireless sensor networks, the traffic pattern may be totally unidirectional [18]. Even for bi-directional traffic scenarios, flows in different directions are not necessarily symmetrical. In some cases, bytes from one direction may account for 85 percent of total traffic [19], so the extra 70 percent traffic from one direction cannot form ANC cooperation due to no flows from the other direction. To keep the performance gain of applying ANC in asymmetrical traffic scenarios, a new design is necessary. Another drawback of the protocol in [17] is that it lacks a mechanism to mitigate the potential issues caused by hidden nodes, which may significantly degrade protocol performance in a multi-hop network [20]. Since the hidden node problem frequently occurs in general mesh/ad hoc networks [21], [22], effective mechanisms are needed to solve this problem.

• W. Mao, X. Wang, and A. Tang are with the University of Michigan-Shanghai Jiao Tong University Joint Institute, Shanghai Jiao Tong University, Shanghai, China. E-mail: wxudong@ieee.org.

• H. Qian is with the Shanghai Institute of Microsystem and Information Technology, Shanghai, China.

Manuscript received 24 June 2014; revised 30 Jan. 2015; accepted 3 Feb. 2015. Date of publication 2 Mar. 2015; date of current version 1 Dec. 2015.

For information on obtaining reprints of this article, please send e-mail to: reprints@ieee.org, and reference the Digital Object Identifier below.

Digital Object Identifier no. 10.1109/TMC.2015.2402122

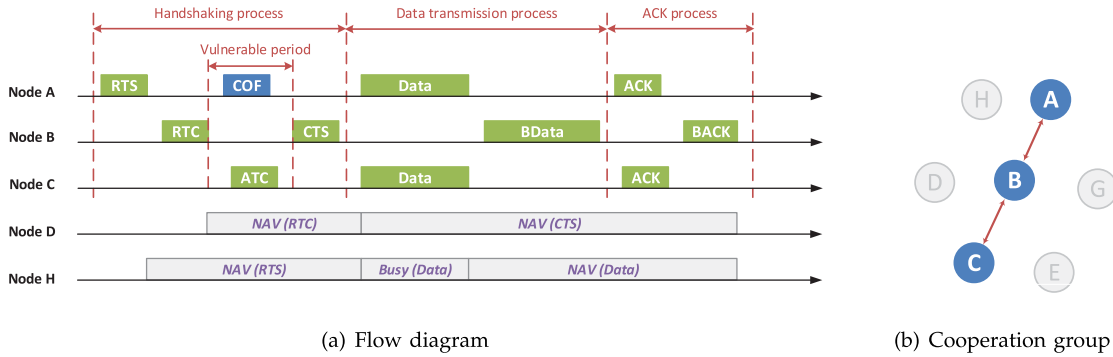


Fig. 1. ANC cooperation in the ANC-ERA protocol.

In this paper, a new MAC protocol is developed to dynamically form ANC cooperation in a wireless network with a general topology. This protocol matches the mechanisms of IEEE 802.11 DCF [23] and enables *Effective Random Access (ERA) of ANC*. Thus, it is called *ANC-ERA*. Specifically, the protocol is characterized by the following distinct features:

- This protocol exploits the short signaling messages (such as RTS/CTS) to dynamically form ANC cooperation groups according to traffic demand, but it does not need the knowledge of queue information of neighboring nodes;
- Several mechanisms are designed to combat issues caused by hidden nodes, which significantly improves protocol performance in a general multi-hop network;
- An effective mechanism is developed to increase ANC cooperation opportunities even if there exists no bi-directional traffic flows.

Both theoretical analysis and simulations are conducted to evaluate the performance of ANC-ERA. Performance results indicate that ANC-ERA works effectively in various situations; as compared to existing schemes, ANC-ERA enhances the network throughput by 5-75 percent and improves the delay performance by 14 percent.

The rest of this paper is organized as follows. In Section 2, the design challenges are presented. The details of our MAC protocol are described in Section 3. The saturation throughput of the protocol is derived in Section 4. In Section 5 the protocol performance is evaluated. The paper is concluded in Section 6.

2 DESIGN CHALLENGES

The primary goal of this paper is to develop a MAC protocol that enables effective random access of ANC in a wireless network with a general topology such as mesh or ad hoc. The challenges to be addressed by this MAC protocol are summarized below:

- To support ANC, cooperation groups need to be formed among different nodes. Considering many nodes in a wireless network, an effective mechanism is needed to form ANC cooperation groups dynamically according to variable traffic demand.
- Compared to traditional point-to-point transmissions, ANC involves a complicated cooperation procedure among multiple nodes. Thus, a network with

ANC cooperation is more vulnerable to hidden nodes. Thus, necessary measures need to be taken to mitigate the impact of this issue on network performance.

- ANC cooperation is well-suited for bi-directional traffic flows between different nodes. However, traffic flows in a network do not always have a symmetrical bid-directional pattern, which reduces the opportunities of forming ANC cooperation. To prevent performance degradation, mechanisms are needed to form ANC cooperation despite of lack of bi-directional traffic flows.

3 ANC-ERA RANDOM ACCESS PROTOCOL

To address the above challenges, a random access MAC protocol called ANC-ERA is designed.

3.1 ANC Cooperation in ANC-ERA

Signaling messages such as RTS and CTS are adopted to form ANC cooperation dynamically. Specifically, the cooperation can be divided into three processes as shown in Fig. 1a. In the handshaking process, different nodes are associated to form cooperation groups according to traffic flows. In the data transmission process, the nodes in the cooperation group send data frames following an ANC scheme. In the ACK process, successful receptions are confirmed. To support ANC cooperation, each node needs to maintain a special neighbor management module in the ANC-ERA protocol.

3.1.1 Neighbor Management Module

Before a node transmits a data frame, it is necessary to determine its one-hop destination and two-hop destination on its routing path¹, for the purpose of ANC cooperation. The one-hop destination information (e.g. MAC and IP address) is already indicated in the routing table, while the two-hop destination information is acquired by maintaining a special neighbor management module in the ANC-ERA protocol. This module utilizes beacon frames to collect necessary neighbor information including routing entries on one-hop neighbors. Based on collected information, a node can gain the knowledge of MAC/IP address of its two-hop neighbors. Moreover, the management module of each

1. In this paper, we assume that the routing is given.

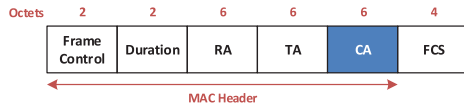


Fig. 2. The format of an RTS frame.

node also maintains a high quality link (HQL) neighbor table, which will be discussed in detail in Section 3.5.

3.1.2 Handshaking Process

Consider Node A (called *initiator*) with a frame that is to be routed through Node B (called *relay*) to Node C (called *cooperator*), as shown in Fig. 1b. As in IEEE 802.11 distributed coordination function (DCF) [23], when the channel is sensed idle and the backoff time counter decreases to zero, Node A sends an RTS frame to initiate the handshaking process. Note that the carrier sensing is only conducted by the initiator before transmitting an RTS frame. Following that, as soon as a node in the cooperation group receives a certain frame correctly, it directly prepares to transmit the subsequent frame (if any) without sensing the channel. The reason behind this design is that when a frame is successfully received by a receiver, it is reasonable to assume that the channel around this receiver is “clean” to some extent, and extra sensing process is not necessary. Similar rule is also adopted by IEEE 802.11 DCF, i.e., the carrier sensing is only carried out by the RTS-sender before transmitting its RTS frame. In addition, to support ANC cooperation, the MAC address of the cooperator (e.g. Node C) is included in this RTS frame by adding a CA field as shown in Fig. 2.

Once the relay (e.g. Node B) successfully receives the RTS frame, it waits for SIFS period, and then transmits an Request-to-Cooperate (RTC) frame to the cooperator (e.g. Node C) as addressed by the RTS frame. The objective of the RTC frame is to request Node C to cooperate with the initiator (e.g. Node A) following an ANC scheme. If Node C has a data frame (called *backward frame*) to send back to the initiator in its transmission queue, it replies an Answer-to-Cooperate (ATC) frame to the relay.

If the relay (e.g. Node B) receives the ATC frame from the cooperator before timeout, it transmits a CTS frame to both the initiator (e.g. Node A) and the cooperator (e.g. Node C). This frame serves as the permission for the ANC cooperation between the initiator and the cooperator. To this end, their addresses are included in the CTS frame by adding an IA field (for initiator) and a CA field (for cooperator) as shown in Fig. 4.

In addition, as shown in Fig. 1a, a channel occupation frame (COF) is sent by the initiator in handshaking process. This frame is designed to avoid channel recapture, as discussed in Section 3.3.

3.1.3 Data Transmission Process

After the initiator and the cooperator receive the CTS frame for ANC cooperation, both transmit their data frames to the

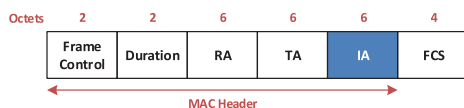


Fig. 3. The format of an ATC frame.

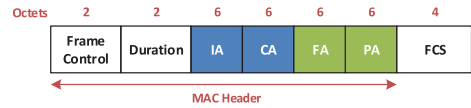


Fig. 4. The format of a CTS frame.

relay after waiting a SIFS time period. Following that, the relay amplifies and forwards the superimposed signals to the initiator and the cooperator as shown in Fig. 1a. With ANC, one node (either the initiator or the cooperator) can decode the data frame from the other node based on the knowledge of its own frame. To support decoding of superimposed signals, each node needs to format its data frame according to the adopted ANC scheme.

3.1.4 ACK Process

If the initiator and the cooperator decode the data frames correctly, they send ACK frames to announce successful receptions. Note that ACK transmission is also conducted in an ANC cooperation manner to improve the communication efficiency, as shown in Fig. 1a. According to the reception status of the corresponding ACK frames, both the initiator and the cooperator update their contention windows and backoff counters following the same process as that in the IEEE 802.11 DCF [23].

3.1.5 Special Cases

If the two-hop destination on the routing path of a data frame does not exist, i.e., the data frame reaches its final destination after the next hop, RTS/CTS and data transmissions follows the same procedure of the IEEE 802.11 DCF. If the relay does not receive any ATC frame before timeout², it presumes that the cooperator does not have a backward frame in its transmission queue. Thus, it sends a CTS to the initiator only (i.e., the CA field is filled with an invalid address). Upon receiving the CTS, the initiator transmits its data frame to the relay following a standard data/ACK procedure.

3.2 Network Allocation Vector Design

In the IEEE 802.11 DCF, the network allocation vector (NAV) of a control frame indicates deferring access until the end of entire transmission processes [23]. However, this design is not suitable for the ANC-ERA protocol as explained below. The transmission process in ANC-ERA involves analog network coding, as shown in Fig. 1a, the NAV duration in a control frame (e.g. RTS or CTS) can be about twice as large as that in DCF. Moreover, the handshaking process in ANC-ERA involves three nodes and four control frames, and the collision of any control frame will lead to failure in handshaking, i.e., the probability of handshaking failure can be higher than that in DCF. Therefore, if the NAV setting of a control frame in ANC-ERA follows the rule of DCF, it will lead to serious *over-blocking* issue, i.e., given a cooperation initiated by control frames, if it fails then all neighbors are prevented from channel access for a long period.

2. The timeout value will be specified in Section 3.5.

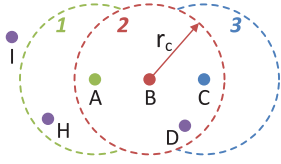


Fig. 5. Channel protection.

Since this issue can significantly degrade the network performance, we propose a new NAV setting for control frames in the ANC-ERA protocol. The NAV of an RTS frame only defers the channel access of neighbor nodes in the period from the end of its transmission to the time when the data frame is sent, as shown in Fig. 1a. Similarly, the NAV of RTC and ATC frames terminates when the data frame transmission starts. The transmission of the CTS frame indicates completion of the handshaking process. To protect the remaining period, the NAV of this type of frame still lasts until the end of entire cooperation process. With this new NAV design, even if the handshaking process fails, the neighboring nodes do not need to wait for more than twice the data frame transmission time before they can access the channel. Thus, the over-blocking issue is significantly alleviated.

The above NAV design does not compromise channel protection. The reason can be explained by looking into different scenarios shown in Fig. 5, where the areas in the dashed circles represent the communication ranges of corresponding nodes.³ First, a node (e.g. Node D) in Region 2 of Fig. 1a will be blocked by the NAV of RTC and CTS frames. Thus, all nodes (except A, B, and C) in this region will definitely defer channel access until the end of the entire cooperation process. Second, the channel access of a node (e.g. Node H) in Region 1 will be deferred by the NAV of the RTS frame, as shown in Fig. 1a. Following that, Node H can sense the data transmission of Node A and hence further defers its channel access. After the data transmission of Node A is complete, thanks to capture effect, Node H can still receive Node A's frame even if Nodes A and C conduct concurrent transmissions. As shown in Fig. 5, the cooperater (i.e., Node C) is always two-hop away from the initiator (i.e., Node A) in a direction opposite to Node H. Thus, the distance between Node A and Node H is much shorter than that between Node C and Node H. Thus, for Node H, the signal strength of the data frame from Node A is much stronger than that from Node C, which enables capture effect [24] at Node H. As a result, Node H can receive the data frame of Node A, in spite of the existence of concurrent transmission from Node C. The NAV in this frame help further defer the channel access of Node H till the end of the entire cooperation process, as shown in Fig. 1a. Similarly, all nodes in Region 3 will be blocked by NAV carried by the ATC frame and the data frame from Node C.

The probability for successful capture depends on the transmission rate of the data frame. For a high transmission rate, corresponding signal-to-interference ratio (SIR) threshold for capture effect is also high. This leads to a lower number of nodes in Region 1 (or Region 3) that can successfully

3. Actually, the communication range of a node is determined by link quality, and is not necessarily a circle.



Fig. 6. New physical-layer format for a data frame.

capture the corresponding data frames, which has negative impact on our scheme. To avoid this issue, a simple but effective scheme is designed as follows. We know that a node in Region 1 (or Region 3) only needs the duration information in the MAC-layer header of the data frame to update its NAV. Based on this observation, we can modify the physical-layer frame format to increase the probability that a node in Region 1 gets the new NAV information, as shown in Fig. 6. In this new format, the *duration symbols* (DS) field is added between physical-layer header (including preamble sequences and important physical-layer parameters, e.g., data rate and frame length) and payload (i.e., the service data unit (SDU) from MAC-layer). The content in the DS field is identical with that in the Duration field of the MAC header [23], but it is coded with 1/2 convolutional coding and modulated with BPSK scheme (i.e., the DS field is transmitted with the base rate), no matter what rate is used to send a MAC frame. With this mechanism, the SIR requirement for capturing the duration information is always identical with that for capturing a data frame with the base transmission rate, i.e., 0 dB as indicated in [24]. Such a SIR can be easily satisfied by a node in Regions 1 and 3, since a node these regions (e.g., Node H) is much closer to its transmitters than to the interfering node.

The overhead introduced by the DS field is low, since the content in this field is identical with that in Duration field of MAC header, which only includes 16 bits [23]. Based on our simulations, the time spent on transmitting the DS field only accounts for 0.7 percent of the total time.

3.3 Channel Occupation Frame

In a wireless network with ANC, the cooperater (e.g. Node C) is two-hop away from the initiator (e.g. Node A). Thus, nodes (e.g. Node D) at the left side of the initiator (as shown in Fig. 5) is even farther from the cooperater and hence may not be able to sense the transmitting signals. In this case, if the initiator takes no action upon receiving an RTC frame, both the initiator and the relay have no transmission until a CTS frame is sent, as shown in Fig. 1a. In this period, nodes such as Node I may sense an idle channel. If Node I is located in the interference range of the initiator, but not in its communication range, Node I cannot receive the RTS frame from the initiator and is thus not blocked by its NAV. In this case, it is possible that Node I sends an RTS frame to capture the channel for new cooperation. If so, the transmission of Node I will interfere the frame reception at Node A, which leads to failure of the ongoing ANC cooperation formed by Nodes A, B, and C. To mitigate this problem, we utilize a channel occupation frame to protect the vulnerable period. As shown in Fig. 1a, after the initiator receives an RTC frame, it transmits a COF, which actually is the RTS frame transmitted previously. In this way, if a node (e.g., Node D) is hidden from the cooperater, but not from the initiator and the relay, it will not sense an idle channel during the entire cooperation process. Even if Node I is also hidden from the relay, the probability that it initiates a new

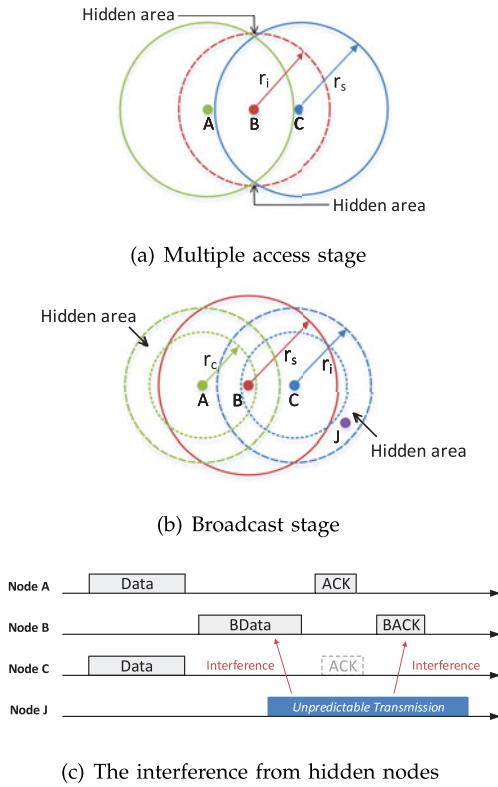


Fig. 7. Hidden nodes in a wireless network with ANC.

transmission during the cooperation process is also significantly reduced, since the continuous channel idle period sensed by Node I becomes much shorter: without COF, it is SIFS+RTC+SIFS+ATC+SIFS+CTS+SIFS; with COF, it is SIFS+RTC+SIFS.

Note that COF may superimpose with the ATC frame at the relay. Since it is the RTS frame transmitted previously, it is known to the relay. Thus, the relay can utilize an analog network coding scheme to cancel the COF frame from the superimposed signals and extract the ATC frame.

3.4 ACK Diversity

3.4.1 The Loss of ACKs

After transmission of an RTS, the remaining ANC cooperation process includes two alternate stages, i.e., multiple access stages and broadcast stages. In a multiple access stage, the initiator and the cooperators concurrently transmit their own frames (e.g. COF/ATC, Datas, ACKs) to the relay, while in a broadcast stage, the relay sends signals (e.g. RTC, BData, BACK) to the initiator and the cooperators. The hidden-node (or hidden-terminal) issues for two stages are illustrated in Figs. 7a and 7b, respectively. In both figures, r_c represents the communication range, r_i stands for the interference range, and r_s denotes the sensing range, and $r_s > r_i > r_c$. Considering a specific pair of transmitter and receiver, usually a region in the interference range of the receiver but outside the sensing range of the transmitter is a hidden area, where a node cannot sense the ongoing transmission(s) but may interfere a receiver with its own transmission. A hidden area in the broadcast stage needs to exclude the area within the communication range of the receiver, because a node in the communication range can

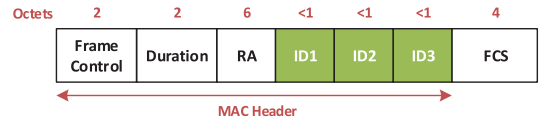


Fig. 8. The format of an ACK frame.

receive a valid NAV due to the capture effect (as explained in Section 3.2).

In a hidden area, a node is not blocked by NAV of either a control or data frame and cannot sense an ongoing transmission. Thus, it may initiate a new transmission and interfere an on-going receiver. As shown in Fig. 7, a hidden area in the multiple access stage is negligible. However, in the broadcast stage a hidden area is much larger, so the hidden-node issue cannot be ignored. This issue becomes more severe when the transmission time in the broadcast stage increases, because nodes in the hidden area have more opportunities to initiate new transmissions. Therefore, in the broadcast stage where the relay amplifies and forwards the superimposed data frames (e.g. BData), a transmission is vulnerable to hidden nodes. If a hidden node (e.g. Node J) starts its transmission in this stage as shown in Fig. 7c, it causes Node C to fail in receiving the BData. Moreover, it is possible that the transmission of Node J further fails the reception of BACK at Node C. In this case, although the data frame from Node C is successfully received by Node A, the ACK (i.e., BACK) is lost. According to simulation studies, occurrence of ACK loss is not rare. For example, when the sensing range is relatively small, about 8.7 percent ACK will be lost. This situation leads to unnecessary retransmissions and degrades network performance. To avoid unnecessary ACK loss, an ACK diversity mechanism is developed in the next section.

3.4.2 ACK Diversity Mechanism

In the ACK diversity mechanism, an ACK frame acknowledges not only the data frame received in the current ANC cooperation but also several data frames that were received recently from the same sender. To support this mechanism, we need to adopt a new format for the ACK frame, allocate IDs for each data frame, and manage a new type of buffers called *ACK-waiting buffer* as explained below.

Frame format. The new format for an ACK frame in the ANC-ERA protocol is shown in Fig. 8. In this frame, ID fields are added, and the number of bits in each field is n_i . The size of n_i depends on the maximum possible ID index, i.e., N_{ID} . The number of ID fields is equal to N_{ACK} . In these fields, IDs for N_{ACK} most recently received data frames from the node indicated by RA field are recorded. In this way, the ID of each received data frame will be carried by N_{ACK} ACKs, i.e., each frame will be acknowledged by N_{ACK} times. This provides N_{ACK} diversity for receiving ACK and hence effectively alleviates the ACK-loss issue.

Data frame ID management. For each data frame, an ID is allocated and specified in the MAC header by adding a new field. To minimize the overhead in ACKs and data frames for carrying IDs, the maximum ID (i.e., N_{ID}) is controlled as small as possible. To this end, different IDs are only used to identify different data frames of the same two-hop destination; The same ID can be used by data frames towards

different destinations, which does not lead to any ambiguity. For each two-hop destination, a node needs to manage the mapping between IDs and data frames towards this destination. To avoid any ambiguity, an ID cannot be allocated to another data frame until the previous data frame with this ID is successfully acknowledged by its receiver, or is discarded when reaching the maximum number of retransmissions.

Buffer management. Under the new ACK scheme, a node needs to manage an ACK-waiting buffer for each two-hop destination. If a transmitted data frame is not acknowledged, it remains in the ACK-waiting buffer instead of being retransmitted immediately. The next data frame in the transmission queue is selected for transmission. Once the ACK for a new transmission is received, the receiver extracts all frame IDs from the ACK. These IDs indicate that corresponding data frames are most recently received by the sender of the ACK. Thus, if the ID of a data frame in the ACK-waiting buffer for this two-hop destination (i.e., the sender of the ACK) appears in the ACK, this frame has been successfully received and can be deleted from the buffer without retransmission. Otherwise, a data frame needs to be moved to the transmission queue for retransmission.

Timeout and delay in retransmission. There actually exist three timers in the ACK-diversity mechanism. First, each transmission is supposed to be acknowledged within a timeout value set in the same way as stop-and-wait ARQ. This is the first timer and its timeout value is set to be the round-trip time from sending a data frame till receiving the corresponding ACK. If the ACK is received before this timer expires, the successful delivery of the data frame is confirmed and it is deleted from the ACK-waiting buffer. However, different from stop-and-wait ARQ, if the timeout of the first timer occurs, the frame retransmission is not triggered immediately. Instead, the next frame in the same transmission queue is sent. As explained before, this mechanism is to reduce unnecessary retransmissions due to ACK loss. However, in order to avoid large delay in retransmitting a lost data frame, two other timers are used to start retransmission of the lost data frame. The second timer is implemented implicitly via a limited size of the ACK-waiting buffer, i.e., whenever the ACK-waiting buffer is exhausted, the least recent frame will be retransmitted. However, it is possible that the ACK-waiting buffer may take a long time to exhaust due to a low frame arrival rate. In this case, the third timer is employed to track the time that a data frame has been staying in the ACK-waiting buffer. The retransmission is triggered if the timeout of the third timer occurs. Thus, this case only occurs when the ACK for a data frame is not received but the arrival rate of new frames is not fast enough to trigger the second timer.

In our design, the ACK-waiting buffer is limited to only three data frames. Thus, retransmission of a lost data frame can be delayed at most two data frames. Moreover, with the buffer size equal to three frames, our scheme can tolerate two consecutive ACK losses without triggering unnecessary retransmissions. According to our simulation, consecutive ACK losses of more than two frames are rarely observed. Thus, the selected buffer size is sufficient for our purpose. The third timer is set to k times of the round-trip time from sending a data frame till receiving the corresponding ACK,

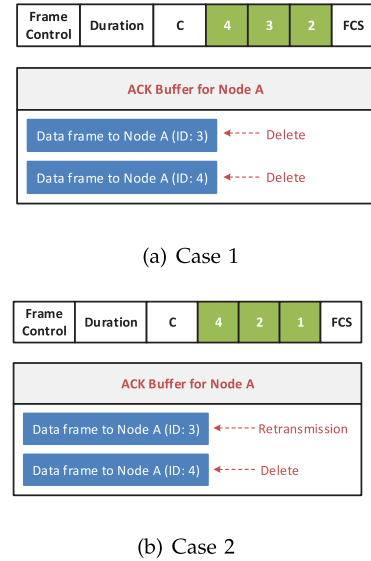


Fig. 9. Buffer management.

where k shall match the size of the ACK-waiting buffer. In our design, k is set to 3.

The ACK-diversity mechanism improves throughput, and the delay performance of our protocol is not compromised much, for two reasons: 1) reducing unnecessary retransmissions due to ACK loss improves throughput and thus reduces delay; 2) the delayed retransmission of a lost data frame is effectively bounded by the second and the third timers.

An example. An example is illustrated in Fig. 9. Consider the ACK-waiting buffer maintained by Node C for a two-hop destination (e.g. Node A). In this buffer, there are two data frames: one is sent in the current ANC cooperation process and its ID equal to 4; the other (with ID equal to 3) is not acknowledged in the previous cooperation process and hence remains in the buffer. Once the ACK in the current cooperation process is received, Node C knows that the data frame sent in this round (i.e., the frame with ID equal to 4) has successfully reached its two-hop destination. Moreover, Node C needs to determine whether the data frame with ID 3 is received by detecting ID fields in this ACK. If ID 3 appears in the ACK as shown in Fig. 9a, Node C knows that the data frame has been successfully received by Node A and deletes it from the buffer directly. Otherwise, as shown in Fig. 9b, Node C knows that the frame is not received and hence moves the frame to the transmission queue for retransmission.

3.5 Flow Compensation

In many cases, the cooperator may not have a data frame to the initiator in its transmission queue when an RTC frame is received, i.e., the traffic between the initiator and the cooperator is not always bi-directional. This traffic pattern is called asymmetric traffic in this paper. In this scenario, an ANC cooperation cannot be formed since the flow from the cooperator is absent. This situation may significantly reduce the probability of forming ANC cooperation and hence has a negative impact on the network performance. Thus, it is critical to develop an effective scheme to maintain performance gain introduced by ANC under such a scenario.

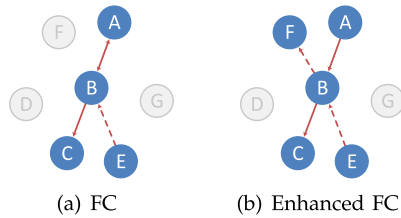


Fig. 10. Flow compensation mechanism (FC).

To this end, a mechanism called *flow compensation* is proposed. As shown in Fig. 10a, if the cooperater does not have a frame to the initiator but one of its neighbors (e.g. Node E) coincidentally has one, the traffic from Node E (called *compensator*) can be used to compensate that from the cooperater (e.g. Node C) to the initiator (e.g. Node A). For this purpose, Node E begins to transmit its data frame after receiving the CTS frame. In this case, the data frames from the initiator (e.g. Node A) and the compensator (e.g. Node E) superimpose at the relay node. Following that, the relay node (e.g. Node B) amplifies and forwards the superimposed signals. With an ANC scheme, Node A can decode the data frame from Node E by cancelling the interference due to its own frame. Also, if the transmission of Node E is successfully overheard, Node C can utilize the ANC scheme to eliminate the interference of the frame from Node E and decode the frame from Node A. Note that overhearing the nearby transmission for cooperation is also investigated in [4], but we are the first to exploit this strategy to solve the asymmetric-traffic problem in a wireless network with ANC.

To apply this mechanism, two problems need to be solved. First, given the cooperater, we need to determine all candidate nodes that can serve as its compensator. These nodes are compensator candidates that have data frames to the initiator. Second, an effective scheme is required to select a certain compensator candidate to form the ANC cooperation (with the initiator). Since each node only has the knowledge about its own queue, a predetermined-based solution is not feasible.

HQL neighbor table. Under the flow compensation mechanism, to decode the initiator's frames, the cooperater needs to overhear the transmission of its compensator successfully. For this purpose, each node maintains a special neighbor table called *high quality link neighbor table*, which contains all neighbors that have high quality links to itself, and its compensator candidates are selected from this table. Given a node, the link quality of its neighbor can be learned from link quality information (e.g. RSSI) contained in frames like beacons, RTS, RTC, etc.

Considering a transmission rate, the threshold for the link quality of the HQL neighbor table is set higher than the minimum received power level for this rate. Since the initiator is two-hop away from the cooperater, the signal from the initiator is much weaker than that from a node in the HQL neighbor table of the cooperater. Thus, the cooperater can successfully overhear the transmission of the node in the HQL neighbor table with high probability. In other words, by tuning the link quality threshold of the HQL neighbor table, we can guarantee that a transmission from a node in this table can be easily captured by the cooperater even under the interference from the initiator. In

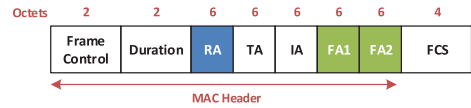


Fig. 11. The format of an RTC frame.

Section 5.2.3, the link quality threshold and the corresponding network performance are studied through experiments.

Note that the signaling overhead due to maintaining the HQL neighbor table is negligible. As explained before, the link quality of a neighbor can be collected from frames sent previously. Moreover, the HQL neighbor table is managed by our neighbor management module as explained in Section 3.1.1. This module utilizes beacon frames to collect the HQL neighbor tables of its adjacent nodes. As a result, maintaining the HQL table does not require extra signaling messages.

Virtual contention for cooperation opportunity. The second problem for applying flow compensation can be solved with virtual contention mechanism. Specifically, after receiving an RTS frame from the initiator, the relay node randomly allocates sequence numbers from 1 to N_c to the compensator candidates, where N_c is the total number of these nodes. The allocation information is carried by the RTC frame by writing the address of candidates following the order of their sequence numbers in the FA fields, as shown in Fig. 11. If N_c is greater than the number of FA fields in an RTC frame, i.e., N_{FA} , the addresses of extra candidates are not written into the RTC frame and hence these nodes are not allowed for transmission in the current cooperation process. Also, the sequence number for the cooperater is always set to zero. The sequence number for each node indicates extra required waiting time for this node before it can start its ATC frame transmission.

Once the RTC is received, the initiator simply starts the transmission of the COF frame after waiting for a SIFS period, while the cooperater and its compensator candidates need to contend the cooperation opportunity according to their sequence numbers. If a node does not have any data frame to the initiator, it simply drops its transmission opportunity. Otherwise, the node will transmit its ATC frame after waiting for $SIFS + n \cdot T_{slot}$, where n is the sequence number for the node and T_{slot} is the slot time. During the waiting time, the node needs to keep overhearing the channel. Once a transmission from the cooperater or other candidates is detected, the node immediately cancels its own transmission attempt to avoid collision as shown in Fig. 12. In this way, only one ATC frame can be successfully sent to the relay and the transmission opportunity is provided to the corresponding node that has data frames to the

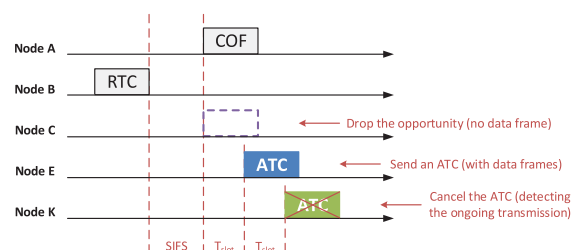


Fig. 12. Flow of frame exchange in different nodes.

initiator. In addition, if none of compensator candidates or cooperators have data frames to the initiator, no ATC frame will be transmitted. This can be determined if the relay fails to receive any ATC frame within $(SIFS + N_{FA} \cdot T_{slot} + ATC)$ after the RTC frame is sent. In this case, a timeout event will be triggered, and a special CTS is sent as described in Section 3.1.5.

Two issues related to the physical-layer design are discussed as follows. First, the transmission of the ATC frame starts at $(SIFS + n \times T_{slot})$ after the end of transmission of the RTC frame. However, the COF frame is sent by the initiator after SIFS period upon receiving the RTC frame. Hence, the COF frame and the ATC frame may superimpose at the relay with a relative delay as large as several slot times, as shown in Fig. 12. To support this situation, ANC schemes that allow frame-level asynchronous transmissions, such as those proposed by [4], [7], are required.

Second, while a compensator candidate is sending an ATC frame, other candidates need to effectively detect the transmission even under the interference (i.e., the COF frame) from the initiator. To this end, ATC frames adopt a different preamble sequence. By correlating this sequence and detecting the correlation peak [25], [26], other candidates can determine whether there exists a transmission of an ATC frame from another candidate.

3.6 Enhanced Flow Compensation

In the scenario shown in Fig. 10a, it is possible that the cooperator and all compensator candidates have no data frames to the initiator, which leads to the failure of forming ANC cooperation. To further increase the probability of forming cooperation, an enhanced flow compensation mechanism is proposed. Under this mechanism, if the cooperator or a compensator candidate (e.g. Node E) has a data frame with the two-hop destination (e.g. Node F) whose HQL-neighbor table includes the initiator, as shown in Fig. 10b, it also attempts to send an ATC frame, following the virtual contention procedure described in Section 3.5. In this ATC frame, the address of the two-hop destination (called *partner*) is carried in the IA field as shown in Fig. 3. To help a node determine if the initiator is included in the HQL neighbor of its certain two-hop destination, a node needs to know HQL-neighbor tables of nodes that are two hops away. This can be realized by our neighbor management module.

Upon receiving such an ATC frame, the relay broadcasts a CTS frame including the addresses of the initiator (in the IA field), the cooperator (in the CA field), the compensator (in the FA field), and the partner (in the PA field), as shown in Fig. 4. In this way, an ANC cooperation is formed as two crossing flows as shown in Fig. 10b. To decode the data frame from the compensator, the partner follows the same strategy with the cooperator as discussed in Section 3.5.

4 PERFORMANCE ANALYSIS

In this section, we derive the saturation throughput that can be achieved by ANC-ERA. As in [27], the throughput is defined as the successfully transmitted payload bits on all links per second. In this paper, saturation means two conditions are satisfied: 1) when the channel is sensed idle, a node always has data frames to send to its two-hop

destinations; 2) when a cooperation request (i.e., an RTC frame) is received, a node always has frames to send back to the initiator.

When hidden nodes exist in a wireless network, throughput analysis is as challenging as deriving the capacity of a wireless network, which is a well-known open research problem. Thus, in this section saturation throughput is only analyzed for a network without hidden nodes. For a multi-hop wireless network with hidden nodes, only simulations are conducted in this paper to evaluate performance of ANC-ERA.

For a network without hidden nodes, we have the following proposition.

Proposition 4.1. *In the ANC-ERA protocol, the saturation throughput of a network with n nodes that can sense each other is given by*

$$\frac{4P_{succ}L_p}{\left(1 - \frac{1}{W_0}\right)T_{slot} + P_{succ}T_s + \left(1 - \frac{1}{W_0}\right)P_{col}T_c},$$

where

$$\begin{cases} P_{succ} = np_t(1 - p_t)^{n-1}, \\ P_{col} = 1 - (1 - p_t)^n - np_t(1 - p_t)^{n-1}, \\ T_s = RTS + SIFS + \delta + RTC + SIFS + \delta + ATC \\ \quad + SIFS + \delta + CTS + SIFS + \delta + BData \\ \quad + SIFS + \delta + BData + SIFS + \delta + BACK \\ \quad + SIFS + \delta + BACK + SIFS + \delta + DIFS, \\ T_c = RTS + DIFS + \delta, \end{cases}$$

and W_0 , T_{slot} , L_p , δ are defined as initial contention window, slot time, payload size in a data frame, and propagation delay, respectively. Also, p_t represents the probability that a node initiates an ANC cooperation process by sending an RTS frame in a given time slot.

The determination of p_t and the proof of the proposition can be found in Appendix A. Based on Proposition 4.1, the saturation throughput can be expressed as

$$\frac{4L_p}{T_s} \cdot \frac{P_{succ}T_s}{\left(1 - \frac{1}{W_0}\right)T_{slot} + P_{succ}T_s + \left(1 - \frac{1}{W_0}\right)P_{col}T_c} = R_{ANC} \cdot \gamma_{ANC}, \quad (1)$$

where R_{ANC} (i.e., $\frac{4L_p}{T_s}$) can be interpreted as the effective transmission rate that has taken into account the overhead introduced by control frames (e.g. RTS and ACK) and frame headers, and γ_{ANC} represents the percentage of time in which the channel is occupied by the successful ANC cooperation process. For comparison, we arrange the expression of the saturation throughput of the IEEE 802.11 DCF derived in [28] into a similar form, i.e., $R_T \cdot \gamma_T$, where R_T is given by $\frac{L_p}{T_s}$ and T_s' denotes the time from the start of sending an RTS to the end of replying ACK under DCF, and γ_T is the counterpart of γ_{ANC} in the DCF case.

Based on the previous discussion, the throughput gain of ANC-ERA over DCF can be divided into two components, i.e., the physical-layer gain (R_{ANC}/R_T) and the MAC-layer gain (γ_{ANC}/γ_T). The physical-layer gain comes from higher spectrum utilization of ANC. If the data transmission rates

TABLE 1
Parameters Used in the Simulation

Parameter	Value	Parameter	Value
MAC header	34 B	RTS	26 B + PH
PHY header (PH)	20 μ s	RTC	38 B + PH
Payload (default)	1,023 B	ATC	26 B + PH
Link rate	54 Mbps	CTS	32 B + PH
Slot time	9 μ s	ACK	15 B + PH
SIFS	16 μ s	α	1
DIFS	34 μ s	Comm. range ¹	1
Max. backoff state	3	Interference range ²	1.78
Init. backoff window (default)	64	Sensing range (default)	2.7
DS	16 bits		

¹The interference range and the sensing range are normalized to the communication range.

²The value is specified according to [30].

under the ANC-ERA protocol and DCF are equal, the time of a successful transmission round in ANC-ERA, i.e., T_s , is about twice as large as its counterpart T'_s in the DCF case. In this scenario, the physical-layer gain, which can be expressed as $4T'_s/T_s$, is close to 2. However, due to the existence of noise accumulation in amplify-and-forward process, the transmission rate with ANC degrades by a factor α ($\alpha \leq 1$), which depends on the SNR and the adopted modulation scheme. Based on the experiments in [7], α is approximately 0.8. If rate degradation is considered, the time for transmitting the same amount of payload increases and leads to a larger T_s . As a result, the physical-layer gain is about 2α .

The other source for the throughput improvement is the MAC-layer gain. Considering the probability (P_{succ}) that an RTS successfully captures the channel in a given time slot, if its value under ANC-ERA is comparable with that under DCF, then the ratio γ_{ANC} is greater than γ_T since T_s is much larger than T'_s . Thus, we expect a MAC-layer gain of greater than 1. In other words, in ANC-ERA the medium is occupied by successful transmissions for a higher proportion of time. This result is confirmed by our simulation, where the MAC-layer gain is approximately 1.1.

5 PERFORMANCE EVALUATION

In this section, performance of ANC-ERA is evaluated through frame-level simulations in Matlab. The simulation programs are event-driven and closely emulate behaviors of our MAC-layer protocol under different scenarios. A node generates data frames to any of its two-hop neighbors as a destination. The generated data frames are cached in a transmission buffer with the capacity equal to 30 frames. Since traditional hop-by-hop forwarding is adopted when ANC cooperation cannot be formed, each node has extra buffer (called *relaying buffer*) for buffering frames that are received from other nodes for forwarding. The size of the relaying buffer at each node is also equal to 30 frames. If the buffers at a node are not empty, the node will initiate transmissions following ANC-ERA. The protocol parameters used in the simulations are based on IEEE 802.11 [23], IEEE 802.11a [29], and our design, and are summarized in Table 1.

Moreover, it is assumed that the link quality is high enough such that the decoding error for any frame is neglected even with noise accumulation caused by ANC (i.e., the factor α mentioned in Section 4 is equal to 1). However, the frame reception fails if there is another transmission in the interference range of the receiver. This range is specified in Table 1. To investigate the protocol performance in various scenarios, our simulation program is applied to two type of networks: 1) two-hop network where hidden nodes do not exist; 2) a general multi-hop network with hidden nodes. In both networks, communication nodes are uniformly distributed in the interested areas.

To compare ANC-ERA with existing schemes, performance of the PNC-MAC proposed in [17] and the IEEE 802.11 DCF [23] is also evaluated. For a fair comparison, all the protocol parameters except control frame sizes are identical in three schemes. The common parameters and the control frame sizes for our protocol are summarized in Table 1, while those for PNC-MAC and DCF are specified in [17] and [23], respectively.

5.1 Performance in Two-Hop Networks

In this part, throughput performance of ANC-ERA protocol is studied in a two-hop network where no hidden node exists. The network size varies from 5 to 50 nodes in our experiments. Under various network sizes, the saturation throughput of ANC-ERA is evaluated based on our simulation programs. For comparison, the performance of PNC-MAC and DCF is also plotted, as shown in Fig. 13. Moreover, the theoretical saturation throughput of ANC-ERA (based on equations in Section 4) and that of DCF (derived in [27]) are also plotted in the figure. It can be observed that the theoretical results of ANC-ERA match well with the simulation results, and the error is less than 1 percent in all cases.

Comparisons also show that the performance gain of ANC-ERA over DCF approaches 114 percent. This significant gain is attributed to two factors. The first factor is the higher spectrum utilization of ANC, which leads to approximately 100 percent throughput improvement, as we assume α is equal to 1. The second factor is the MAC-layer efficiency. In fact, MAC-layer efficiency depends on two types of overhead introduced by MAC protocols.

The first type is the control frame overhead, i.e., the time spent on transmitting MAC-layer control frames. When the data frame size is equal to 1,023 bytes, the control frame overhead of ANC-ERA is around 20 percent of the total time, while that of DCF is close to 17 percent. When the data frame size decreases, the overhead increases, but so does DCF. The protocol performance with different frame sizes will be studied in a multi-hop network in Section 5.2.2.

The second type is the channel access overhead, i.e., time spent on channel contention, backoff, DIFS/SIFS, and etc. In ANC-ERA, the channel access overhead is about 30 percent of the total time, while that in DCF is around 36 percent. The reason for lower channel access overhead in our protocol is as follows: for each successful channel access, the data transmission time in ANC-ERA is much longer than that in DCF, so the overhead caused by contention and backoff

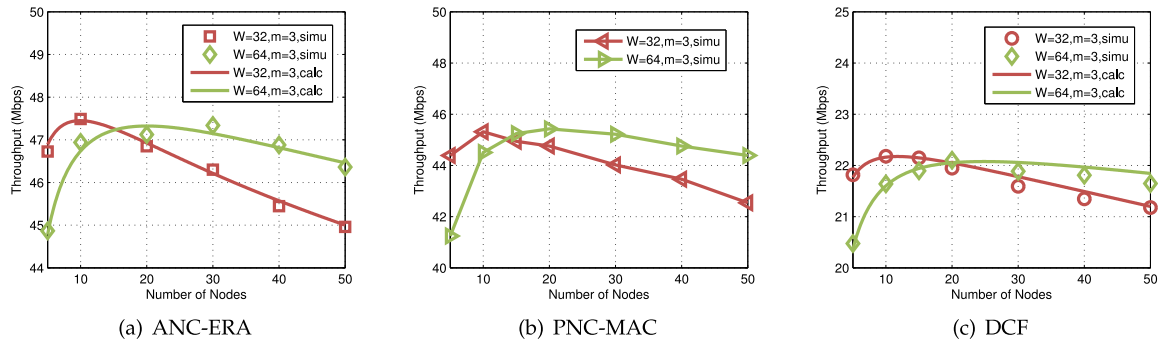


Fig. 13. Saturation throughput in a two-hop network.

accounts for a lower proportion. Considering two types of overhead jointly, we know that the MAC-layer efficiency of our protocol is higher.

Compared to PNC-MAC protocol, ANC-ERA has approximately 5 percent throughput gain. This advantage is due to the more efficient ACK process in our protocol, as the transmission of ACK is also conducted in an ANC cooperation manner.

In addition, it can be observed that the throughput of our protocol first increases and then goes down as the number of nodes increases, similar with the cases of DCF and PNC-MAC. The increase of the throughput performance is attributed to the better utilization of wireless medium, while the decrease is due to the more intensive channel contention. Moreover, although these results are based on the saturated cases, similar trends can be observed in unsaturated scenarios.

5.2 Performance in General Multi-Hop Networks

The protocol performance is evaluated in a general multi-hop network with 300 communication nodes. The network is deployed in the area with the size 10×10 (normalized to the communication range). The hidden nodes in this network significantly impact protocol performance.

5.2.1 Mechanisms for Combating Hidden Nodes

First, we evaluate the proposed mechanisms for combating hidden nodes. These mechanisms include NAV enhancement, channel occupation frame, and ACK diversity. To understand their performance gains under various amount of hidden nodes, we evaluate the protocol with different sensing ranges: shorter sensing ranges lead to more hidden nodes, while longer sensing ranges reduce the amount of them. Since the relation between hidden nodes and sensing ranges is uncorrelated to the traffic load (saturated or not),

we present the results based on saturated scenarios and similar observations hold for unsaturated cases.

NAV enhancement. To evaluate the effectiveness of new NAV setting, we compare the performance of the ANC-ERA protocol with and without NAV modification, as shown in Fig. 14. It can be observed that the ANC-ERA protocol with NAV modification significantly outperforms the protocol without NAV modification.

In these experiments, nodes in Regions 1 and 3 (see Fig. 5) can always capture the NAV information from corresponding data frames. This assumption is valid as explained in Section 3.2.

Channel occupation frame. The network throughput of ANC-ERA with and without COF is compared under various sensing ranges, as shown in Fig. 15. Results show that the throughput performance of the protocol degrades when COF is disabled. The reason is that cooperation groups are not effectively protected without COF, which leads to failure of ANC cooperation. As the sensing range increases, hidden nodes that cause this problem become rare, and thus cooperation groups do not need protection from COF. As a result, the performance gap between two cases diminishes when the sensing range reaches 2.7 (normalized to communication range). Moreover, in our simulation, the transmission rate is set to 54 Mbps. If a low transmission rate is adopted, the length of an ATC frame becomes longer and so does the vulnerable period as specified in Fig. 1a. In this situation, COF is more critical.

ACK diversity. The ACK loss rates under various schemes are summarized in Table 2. It shows that the DCF scheme is free from the ACK loss issue. In contrast, in a network with ANC cooperation, a fraction of ACK frames are not received, although the corresponding data frames have arrived at their destinations. Moreover, as the sensing range decreases, the hidden-node issue results in higher ACK

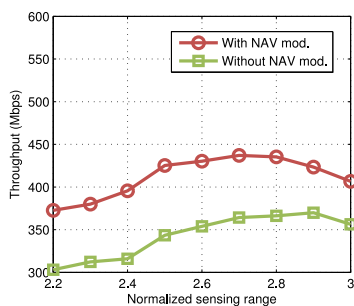


Fig. 14. Throughput versus NAV (1,023-byte frame).

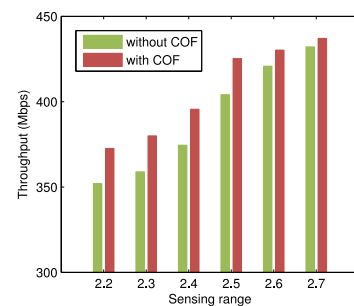


Fig. 15. Throughput performance with/without COF.

TABLE 2
ACK Loss Rates under Various Schemes

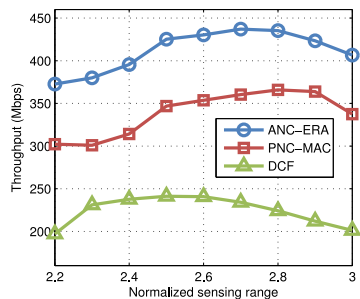
Sensing range	DCF	ANC-ERA	
		w/o ACK diversity	with ACK diversity
2.2	~ 0	8.71%	0.20%
2.4	~ 0	7.63%	0.13%
2.6	~ 0	4.58%	~ 0
2.8	~ 0	2.80%	~ 0

loss. When the ACK diversity mechanism is applied, the results in Table 2 show that the probability of ACK loss is dramatically reduced.

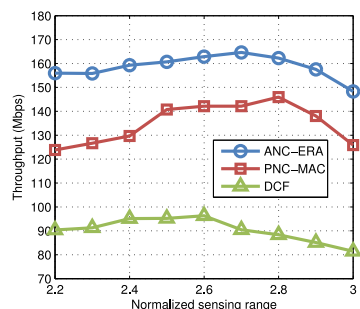
5.2.2 Saturation Throughput

Saturation throughput of the ANC-ERA protocol in a general multi-hop network is shown in Fig. 16, where two scenarios are considered: frame sizes of 1,023 and 256 bytes. For comparison, the performance of PNC-MAC and DCF is also provided. With a frame size of 1,023 bytes (i.e., in Fig. 16a), the throughput of the ANC-ERA protocol is approximately 81 percent better than that of the DCF scheme, which is lower than the performance gain in the two-hop network case. This is because a network with ANC cooperation is more vulnerable to hidden nodes as compared to a network with traditional point-to-point transmissions. Also, results show that the throughput of ANC-ERA is 20-25 percent higher than that of PNC-MAC. This performance gain is achieved by our solutions to the over-blocking issue, the channel recapture issue, and the ACK loss issue as discussed in Sections 3.2, 3.3, and 3.4.1, respectively. All these issues exist in the PNC-MAC protocol.

When the frame size drops to 256 bytes (i.e., in Fig. 16b), the throughput is much lower than the case of large frame



(a) frame size: 1023 bytes



(b) Frame size: 256 bytes

Fig. 16. Saturation throughput in a multi-hop network.

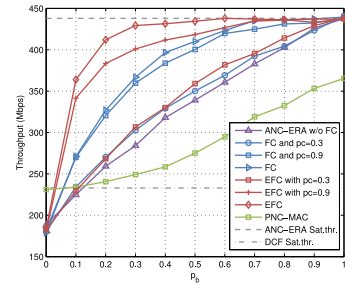


Fig. 17. Throughput performance versus p_b under various p_e .

size. However, the performance advantage of our protocol over other protocols is still maintained. Note that it is reasonable that the throughput drops as frame size decreases due to increasing overhead.

5.2.3 Throughput Performance in Unsaturated Cases

In many scenarios, the cooperators do not necessarily have a backward frame toward the initiator when the ANC cooperation request (an RTC frame) arrives. Thus, it is meaningful to evaluate our protocol in an unsaturated mode. To characterize this situation, we define p_b as the probability that one node (e.g., the cooperator or the compensator candidates) has backward frames to its certain two-hop neighbor (e.g., the initiator) when an RTC frame is received. The throughput performance of our protocol with flow compensation mechanisms is evaluated under various p_b . In these experiments, an RTC frame contains two FA fields as shown in Fig. 11. Hence, at most two compensator candidates can be exploited in our evaluations. For comparison, the performance of PNC-MAC and DCF is also evaluated. The results are shown in Fig. 17.

It can be observed that the throughput performance of ANC-ERA is slightly lower than that of DCF when p_b is close to zero. In this case, no ATC frame will be received by the relay, and thus traditional data/ACK procedure is proceeded between the initiator and the relay as mentioned in Section 3.1.5. If so, our protocol degenerates to a traditional CSMA/CA protocol but with longer handshaking process. Thus, its performance is lower than that of DCF. For PNC-MAC, if there is no cooperation opportunity, only traditional transmission procedure is triggered. Thus, when p_b is close to zero, its performance is nearly identical to that of DCF.

Moreover, when p_b is greater than zero, the throughput performance of ANC-ERA with the flow compensation mechanism (labeled by "FC") and the extended FC mechanism (EFC) increases more rapidly as compared to ANC-ERA without these mechanisms (ANC-ERA w/o FC) or PNC-MAC. When p_b is equal to 0.2, the performance gain of ANC-ERA (with EFC) over PNC-MAC reaches 75 percent. This significant improvement is achieved thanks to FC mechanisms, as they enable more ANC cooperations. In this case, backward flows can be provided not only by the cooperator but also by all potential compensators.

Under the FC mechanism, the cooperator is required to overhear the frame from the compensator. In previous evaluations, we assume that the overhearing is always perfect. However, it is possible that the cooperator fails to capture the compensator's frames, and hence cannot decode the

TABLE 3
The Capture Probability p_c for Different Transmission Rates

Transmission Rate (Mbps)	p_c ($d_{DC} \leq r_c$)	p_c ($d_{DC} \leq \frac{1}{2}r_c$)	p_c ($d_{DC} \leq \frac{1}{3}r_c$)
54	0.13	0.47	0.79
24	0.61	0.97	1.00
9	0.75	0.99	1.00

frame sent by the initiator. This has negative impact on the throughput performance. Under EFC, both directions in an ANC cooperation involve overhearing, and the impact of overhearing failure on the performance is even larger. To investigate the performance under imperfect overhearing, we evaluate our protocol under various capture probability p_c , i.e., the probability that the overhearing is successful.

The throughput performance of our protocol under various p_c is shown in Fig. 17. It can be observed that when p_c is equal to 0.9, the protocol performance closely follows the case of perfect capture. The performance gap is at most 3.3 percent under the FC mechanism and 6.9 percent under the EFC mechanism. When p_c drops to 0.3, the performance seriously degrades as compared to the case of perfect capture, but is still better than that without FC mechanisms. In this case, the benefit from FC mechanisms (i.e., more ANC cooperation opportunities) is largely neutralized by the negative impact of overhearing failure.

p_c versus link quality threshold of a HQL Table. As previous results indicate, the performance of the protocol largely depends on the capture probability p_c . This probability is highly related to the transmission rate: the higher the rate, the lower the capture probability. To increase p_c for high transmission rates, we can set a higher link quality threshold for the HQL neighbor table. This requires the knowledge about the relationship between p_c and link quality threshold.

To investigate this relationship, a simulation is conducted as follows. Considering three nodes in a two-hop setup (like A-B-C), Node A is the initiator, Node B is the relay, and Node C is the cooperater. The fourth node D is then randomly placed into a certain range of Node C. The channel attenuation index is assumed to be 3 and Rayleigh fading is considered. Let Node D and Node A transmit with the same power level at the same time, and we then check if Node C can receive Node D's frame. For the sake of clarity, the link quality threshold of a HQL neighbor table is represented by the range where its member (e.g. Node D) can be located. If Node D is located in anywhere of the Node C's communication range, then it means the link quality threshold is set to the minimum value and all neighbors belong to the HQL neighbor table. To increase the link quality threshold, the range of Node D's locations is reduced to a smaller value. Under each range, we vary Node D's locations and then collect the statistics of Node C's overhearing results, which reveals the successful overhearing probability, i.e., p_c .

For different transmission rates, the results of p_c under various link quality thresholds are shown in Table 3, where d_{DC} is the distance between Nodes D and C, and r_c is the communication range of Node C (which varies with the transmission rate). As shown in Table 3, if we increase the link quality threshold (as represented by the decreasing

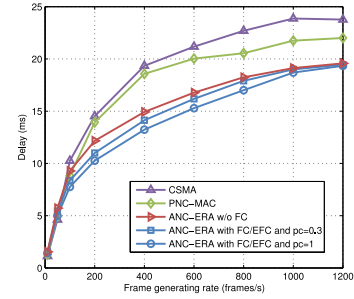


Fig. 18. Delay performance of different schemes.

range of d_{DC}), then p_c is much improved. Even under the rate of 54 Mbps, p_c can reach 0.79 when the threshold is set to 1/3 of the communication range.

Note that a higher link quality threshold leads to a smaller HQL neighbor table. In a sparse network, this may reduce the number of compensator candidates and hence the opportunities for ANC cooperations, which has negative impact on the network performance. Thus, the selection of the link quality threshold also need to take the sparsity of the network into account.

5.2.4 Delay Performance

The delay performance of ANC-ERA is also evaluated under an unsaturated mode. The delay refers to the period from the time when a data frame arrives in a transmission buffer till the frame is received by its two-hop destination. Moreover, the frame generation rate varies from 10 frames per second to 1,200 frames per second. The results of delay versus various frame generating rates are shown in Fig. 18. It can be observed that the delay of our scheme is evidently lower than that of PNC-MAC. This enhancement is attributed to two factors. First, the improved throughput performance is beneficial to enhance the departure rate of a buffer at each node. Second, when the frame generation rate is low, the cooperater may not always have a frame to the initiator. In this case, FC mechanisms in our protocol significantly increase the opportunity of forming ANC cooperation. When an ANC cooperation is formed, two frames sent to their two-hop destinations do not enter the buffer of the relay node, which effectively avoids extra queuing delay at the relay node.

In addition, we also evaluate the relationship between overhearing failure and the delay performance. When the capture probability is low (e.g., $p_c = 0.3$ as shown in Fig. 18), the delay performance degrades. However, the degradation is not significant, and the performance is still better than that without FC mechanisms.

6 CONCLUSION

In this paper, a random access MAC protocol called ANC-ERA was developed to support ANC in a general wireless network. Several mechanisms, such as the NAV enhancement, the channel occupation frame, and the ACK diversity, were designed to combat issues caused by the hidden-node issue in a network with ANC cooperation. Moreover, the protocol includes an effective mechanism to enable ANC cooperation even if bi-directional traffic flows between ANC nodes are absent. This distinct feature eliminates the

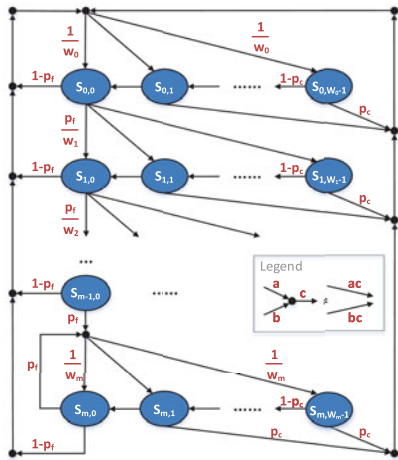


Fig. 19. The Markov chain for backoff state transitions.

dependence of ANC on traffic patterns, and significantly extends the application scope of ANC. The performance of ANC-ERA was evaluated by both theoretical analysis and network simulations. Results showed that ANC-ERA significantly outperforms existing schemes. Throughput analysis of ANC-ERA in a general network is subject to future research.

APPENDIX A PROOF OF PROPOSITION 4.1

Consider a network with n nodes that can sense each other. For each node, it may stay in different backoff stages. The contention window for the i th backoff stage is denoted by W_i , where i is a non-negative integer and bounded by a constant m . A node in the i th backoff stage has a backoff counter in the range $[0, W_i - 1]$. To characterize backoff of each node, we use $S_{i,j}$ to denote the state that a node enters the i th backoff stage and has a backoff counter equal to j .

There exist two important probabilities affecting transitions between different states $\{S_{i,j}\}$. One is the transmission failure probability p_f , which is defined as the probability that collision happens in an ANC cooperation process and leads to the failure of ANC cooperation. As mentioned in [27], it is reasonable to assume p_f to be independent from the number of retransmissions. The other key probability is the cooperation probability p_c , defined as the probability that one node receives a cooperation request (i.e., an RTC frame) when it stays in a backoff state and forms ANC cooperation with the initiator. Note that the cooperation probability is independent from backoff stages and counters.

Based on the above definitions, we can model the transitions between states $\{S_{i,j}\}$ as a discrete-time Markov chain. As shown in Fig. 19, all of non-zero state transition probabilities are:

$$\begin{cases} p\{S_{0,j}|S_{i,0}\} = \frac{1-p_f}{W_0}, i \in [0, m], j \in [0, W_0) \\ p\{S_{i+1,j}|S_{i,0}\} = \frac{p_f}{W_{i+1}}, i \in [0, m), j \in [0, W_{i+1}) \\ p\{S_{m,j}|S_{m,0}\} = \frac{p_f}{W_m}, j \in [0, W_m) \\ p\{S_{0,k}|S_{i,j}\} = \frac{p_c}{W_0}, i \in [0, m], j \in [0, W_i), k \in [0, W_0) \\ p\{S_{i,j-1}|S_{i,j}\} = 1 - p_c, i \in [0, m], j \in [1, W_i), \end{cases} \quad (2)$$

The first three equations in (2) represent backoff behaviors after collisions or successful transmissions, which is similar to the case in the IEEE 802.11 DCF. The fourth equation describes the state transitions due to the data transmission as a cooperator. Specifically, if a node receives an RTC frame, under saturation conditions, it always has a data frame to the initiator and ANC cooperation will be formed. Since the channel has been captured by the RTS frame and all nodes can sense the ongoing transmission, the data frames sent by the initiator and the cooperator will be free from collisions and can be successfully received. In this case, the node resets its backoff stage to zero and takes a random backoff, i.e., the backoff state will be changed following the probability in the fourth equation. The last equation indicates that, if a node does not receive any cooperation request, it will reduce its backoff counter slot by slot, once the channel is sensed idle for a DIFS period.

Let $\{v_{i,j}\}$ denote the stationary distribution of $\{S_{i,j}\}$. It can be shown that

$$\begin{cases} v_{0,j} = v_{0,j+1}(1 - p_c) + \frac{v_c p_c}{W_0} + v_t \frac{1-p_f}{W_0}, j \in [0, W_0) \\ v_{i,j} = v_{i,j+1}(1 - p_c) + \frac{v_{i-1,0} p_f}{W_i}, i \in [1, m), j \in [0, W_i) \\ v_{m,j} = v_{m,j+1}(1 - p_c) + \frac{v_{m-1,0} p_f}{W_m} + \frac{v_{m,0} p_f}{W_m}, j \in [0, W_m) \\ \sum_{i=0}^m \sum_{j=0}^{W_i-1} v_{i,j} = 1, \end{cases} \quad (3)$$

where

$$v_c = \left(\sum_{i=0}^m \sum_{j=1}^{W_i-1} v_{i,j} \right), \quad v_t = \sum_{i=0}^m v_{i,0}. \quad (4)$$

Based on Eq. (3), we can prove that

$$v_{i,0} = \frac{p_f^i [v_c p_c + v_t (1 - p_f)]}{p_c^{i+1} \delta_i} \prod_{k=0}^i \frac{1 - (1 - p_c) W_k}{W_k},$$

where δ_i is given by

$$\begin{cases} \frac{p_c W_m - p_f [1 - (1 - p_c) W_m]}{p_c W_m}, & i = m \\ 1, & \text{otherwise.} \end{cases}$$

Then, according to Eq. (4), v_t can be expressed as

$$v_t = [v_c p_c + v_t (1 - p_f)] \left\{ \sum_{i=0}^m \frac{p_f^i}{p_c^{i+1} \delta_i} \prod_{k=0}^i \frac{1 - (1 - p_c) W_k}{W_k} \right\}.$$

We define the expression inside braces in the above equation as $c(p_f, p_c)$. From Eq. (4) and Eq. (3), we also know that $v_c + v_t = 1$. Thus, it can be shown that

$$v_t = \frac{c(p_f, p_c) p_c}{1 - c(p_f, p_c) (1 - p_c - p_f)}.$$

Furthermore, the transmission probability p_t is defined as the probability that a node initiates an ANC cooperation process in a given time slot. Thus, it can be expressed as

$$p_t = \sum_{i=0}^m v_{i,0} = v_t = \frac{c(p_f, p_c) p_c}{1 - c(p_f, p_c) (1 - p_c - p_f)}. \quad (5)$$

For the sake of simplicity, we consider a symmetric setting where each node has an equal opportunity to participate in an ANC cooperation. In this case, we can assume that the cooperation probability p_c is the same for all nodes in the network. Also, as mentioned in [27], it is reasonable to assume that p_f keeps invariant for different nodes. Furthermore, since the transmission probability is determined by the cooperation probability p_c and the transmission failure probability p_f , we conclude that the transmission probability p_t is also invariable over nodes.

Let D_X denote the set of nodes that have data frames with Node X as their two-hop destination and T_X represent the set of nodes which are two-hop destinations of data frames from Node X. Also, p_{XY}^t stands for the probability that Node X transmits an RTS frame with Node Y as the two-hop destination in a given time slot, and p_{XY}^s denotes the probability that such an RTS frame is free from collision and captures the channel. Thus, for a specific station A, the cooperation probability is given by

$$p_c = \sum_{X \in D_A} p_{XA}^t p_{XA}^s = (1 - p_t)^{n-2} \sum_{X \in D_A} p_{XA}^t.$$

Adding the cooperation probabilities of all nodes together, we have that

$$\begin{aligned} \sum_Y p_c &= (1 - p_t)^{n-2} \sum_Y \sum_{X \in D_Y} p_{XY}^t \\ &= (1 - p_t)^{n-2} \sum_X \sum_{Y \in T_X} p_{XY}^t \\ &= (1 - p_t)^{n-2} \sum_X p_t. \end{aligned}$$

We know that p_c and p_t are same for all nodes, so

$$p_c = p_t (1 - p_t)^{n-2}. \quad (6)$$

Moreover, the transmission failure probability is

$$p_f = 1 - (1 - p_t)^{n-1}. \quad (7)$$

Combining Eqs. (5), (6), and (7), we can derive p_t , p_f and p_c with a numerical method. The above derivation is based on symmetric setting of traffic patterns. However, our theoretical framework can be applied to a general scenario where p_t , p_f and p_c vary for different nodes, so we need to solve $3n$ equations to obtain these probabilities.

With the above probabilities, the saturation throughput can be calculated following similar steps in [28]. The main difference is that each successful ANC cooperation delivers two data frames for two end nodes that are two-hop away, which is equivalent to four transmissions in a network based on the IEEE 802.11 DCF. The saturation throughput is given in Proposition 4.1.

ACKNOWLEDGMENTS

The research work is supported by National Natural Science Foundation of China (NSFC) No. 61172066 and Oriental Scholar Program of Shanghai Municipal Education Commission. The authors would like to thank these sponsors for their generous support. Xudong Wang is the corresponding author.

REFERENCES

- [1] P. Popovski and H. Yomo, "Bi-directional amplification of throughput in a wireless multi-hop network," in *Proc. IEEE 63rd Veh. Technol. Conf.*, 2006, pp. 588–593.
- [2] S. Zhang, S. C. Liew, and P. P. Lam, "Hot topic: Physical-layer network coding," in *Proc. ACM 12th Annu. Int. Conf. Mobile Comput. Netw.*, 2006, pp. 358–365.
- [3] B. Rankov and A. Wittneben, "Spectral efficient protocols for half-duplex fading relay channels," *IEEE J. Sel. Areas Commun.*, vol. 25, no. 2, pp. 379–389, Feb. 2007.
- [4] S. Katti, S. Gollakota, and D. Katabi, "Embracing wireless interference: Analog network coding," in *Proc. ACM Conf. Appl., Technol., Archit. Protocols Comput. Commun.*, 2007, pp. 397–408.
- [5] F. Rossetto and M. Zorzi, "On the design of practical asynchronous physical layer network coding," in *Proc. IEEE 10th Workshop Signal Process. Adv. Wireless Commun.*, 2009, pp. 469–473.
- [6] L. Lu, S. C. Liew, and S. Zhang, "Optimal decoding algorithm for asynchronous physical-layer network coding," in *Proc. IEEE Int. Conf. Commun.*, 2011, pp. 1–6.
- [7] X. Wang and W. Mao, "Analog network coding without restrictions on superimposed frames," *IEEE/ACM Trans. Netw.*, Digital Object Identifier: 10.1109/TNET.2014.2385857.
- [8] S. Fu, K. Lu, T. Zhang, Y. Qian, and H.-H. Chen, "Cooperative wireless networks based on physical layer network coding," *IEEE Trans. Wireless Commun.*, vol. 17, no. 6, pp. 86–95, Dec. 2010.
- [9] J. H. Sørensen, R. Krigslund, P. Popovski, T. K. Akino, and T. Larsen, "Scalable noise-and-forward in bidirectional relay networks," *Comput. Netw.*, vol. 54, no. 10, pp. 1607–1614, 2010.
- [10] I. Maric, A. Goldsmith, and M. Médard, "Multihop analog network coding via amplify-and-forward: the high SNR regime," *IEEE Trans. Inf. Theory*, vol. 58, no. 2, pp. 793–803, Feb. 2012.
- [11] K. Jitvanichphaibool, R. Zhang, and Y.-C. Liang, "Optimal resource allocation for two-way relay-assisted OFDMA," *IEEE Trans. Veh. Technol.*, vol. 58, no. 7, pp. 3311–3321, Sep. 2009.
- [12] A. Argyriou and A. Pandharipande, "Cooperative protocol for analog network coding in distributed wireless networks," *IEEE Trans. Wireless Commun.*, vol. 9, no. 10, pp. 3112–3119, Oct. 2010.
- [13] H. Su and X. Zhang, "Modeling throughput gain of network coding in multi-channel multi-radio wireless ad hoc networks," *IEEE J. Sel. Areas Commun.*, vol. 27, no. 5, pp. 593–605, Jun. 2009.
- [14] O. Goussevskaia and R. Wattenhofer, "Complexity of scheduling with analog network coding," in *Proc. ACM 1st ACM Int. Workshop Found. Wireless Ad Hoc Sensor Netw. Comput.*, 2008, pp. 77–84.
- [15] M. Khabbazian, F. Kuhn, N. Lynch, M. Médard, and A. ParandehGheibi, "MAC design for analog network coding," in *Proc. ACM 7th ACM ACM SIGACT/SIGMOBILE Int. Workshop Found. Mobile Comput.*, 2011, pp. 42–51.
- [16] A. Argyriou, "MAC protocol for wireless cooperative physical-layer network coding," in *Proc. IEEE Wireless Commun. Netw. Conf.*, 2012, pp. 1596–1601.
- [17] S. Wang, Q. Song, X. Wang, and A. Jamalipour, "Distributed MAC protocol supporting physical-layer network coding," *IEEE Trans. Mobile Comput.*, vol. 12, no. 5, pp. 1023–1036, May 2013.
- [18] G. Lu, B. Krishnamachari, and C. S. Raghavendra, "An adaptive energy-efficient and low-latency MAC for data gathering in wireless sensor networks," in *Proc. IEEE 18th Int. Parallel Distrib. Process. Symp.*, 2004.
- [19] G. Maier, A. Feldmann, V. Paxson, and M. Allman, "On dominant characteristics of residential broadband internet traffic," in *Proc. ACM SIGCOMM*, 2009.
- [20] F. A. Tobagi and L. Kleinrock, "Packet switching in radio channels: Part II—the hidden terminal problem in carrier sense multiple-access and the busy-tone solution," *IEEE Trans. Commun.*, vol. 23, no. 12, pp. 1417–1433, Dec. 1975.
- [21] K. Xu, M. Gerla, and S. Bae, "How effective is the IEEE 802.11 rts/cts handshake in ad hoc networks," in *Proc. IEEE Global Telecommun. Conf.*, 2002, pp. 72–76.
- [22] I. F. Akyildiz and X. Wang, "A survey on wireless mesh networks," *IEEE Commun. Mag.*, vol. 43, no. 9, pp. S23–S30, Sep. 2005.
- [23] IEEE, *IEEE Standard for Information Technology—Telecommunications and Information Exchange Between Systems—Local and Metropolitan Area Networks—Specific Requirements—Part 11: Wireless LAN Medium Access Control (MAC) and Physical Layer (PHY) Specifications*, IEEE Std 802.11-2007, pp. 72–74, 2007.

- [24] J. Lee, W. Kim, S.-J. Lee, D. Jo, J. Ryu, T. Kwon, and Y. Choi, "An experimental study on the capture effect in 802.11a networks," in *Proc. ACM 2nd Int. Workshop Wireless Netw. Testbeds, Exp. Evaluation Characterization*, 2007, pp. 19–26.
- [25] S. Gollakota and D. Katabi, "Zigzag decoding: Combating hidden terminals in wireless networks," in *Proc. ACM SIGCOMM*, 2008, pp. 159–170.
- [26] K. Tan, H. Liu, J. Fang, W. Wang, J. Zhang, M. Chen, and G. M. Voelker, "SAM: Enabling practical spatial multiple access in wireless LAN," in *Proc. ACM 15th Annu. Int. Conf. Mobile Comput. Netw.*, 2009, pp. 49–60.
- [27] G. Bianchi, "Performance analysis of the IEEE 802.11 distributed coordination function," *IEEE J. Sel. Areas Commun.*, vol. 18, no. 3, pp. 535–547, Mar. 2000.
- [28] G. Bianchi and I. Tinnirello, "Remarks on IEEE 802.11 DCF performance analysis," *IEEE Commun. Lett.*, vol. 9, no. 8, pp. 765–767, Aug. 2005.
- [29] *IEEE, Part 11: Wireless LAN medium access control (MAC) and physical layer (PHY) specifications: High-speed physical layer in the 5 GHz band*, IEEE Std 802.11a-1999, p. 24, 1999.
- [30] F. Ye, S. Yi, and B. Sikdar, "Improving spatial reuse of IEEE 802.11 based ad hoc networks," in *Proc. IEEE Global Telecommun. Conf.*, 2003, pp. 1013–1017.



Wenguang Mao received the BS degree in electrical and computer engineering from Shanghai Jiao Tong University (SJTU), Shanghai, China, in 2011 and the MS degree in information and communication engineering from SJTU in 2014. His current research interests include MAC protocols, physical-layer cooperative coding schemes, and mobile applications in smart phones and wearable computers.



Xudong Wang received the PhD degree in electrical and computer engineering from the Georgia Institute of Technology in August 2003. Since then he has been working as a senior research engineer, senior network architect, and R&D manager in several US companies. He is currently with the UM-SJTU Joint Institute, Shanghai Jiao Tong University. He is a distinguished professor (Shanghai Oriental Scholar) and is the director of the Wireless and NetworkinG (WANG) Lab. He is also an affiliate faculty member with

the Electrical Engineering Department at the University of Washington. He has been actively involved in R&D, technology transfer, and commercialization of various wireless networking technologies. His research interests include wireless communication networks, smart grid, and cyber physical systems. He holds several patents on wireless networking technologies and most of his inventions have been successfully transferred to products. He is an editor for *IEEE Transactions on Mobile Computing*, *IEEE Transactions on Vehicular Technology*, Elsevier *Ad Hoc Networks*. He was the demo co-chair of the ACM International Symposium on Mobile Ad Hoc Networking and Computing (ACM MOBIHOC 2006), a technical program co-chair of Wireless Internet Conference (WICON) 2007, and a general co-chair of WICON 2008. He has been a technical committee member of many international conferences. He is a senior member of the IEEE.



Aimin Tang received the BS degree in electrical and computer engineering from Shanghai Jiao Tong University (SJTU), Shanghai, China, in 2013. He is currently working towards the PhD degree with the Wireless and Networking Lab at the University of Michigan-Shanghai Jiao Tong University Joint Institute. His current research interests include full duplex communications, rateless coding, and software defined wireless networks.



Hua Qian received the BS and MS degrees from the Department of Electrical Engineering, Tsinghua University in 1998 and 2000, respectively, and the PhD degree from the School of Electrical and Computer Engineering, Georgia Institute of Technology in 2005. He is currently with Shanghai Research Center for Wireless Communications, Shanghai Institute of Microsystem and Information Technology Research Institute, Chinese Academy of Sciences as a full professor. His current research interests include nonlinear signal processing and system design of wireless communications.

▷ For more information on this or any other computing topic, please visit our Digital Library at www.computer.org/publications/dlib.